

Coibamide A Targets Sec61 to Prevent Biogenesis of Secretory and Membrane Proteins

Dale Tranter,[#] Anja O. Paatero,[#] Shinsaku Kawaguchi, Soheila Kazemi, Jeffrey D. Serrill, Juho Kellosalo, Walter K. Vogel, Uwe Richter, Daphne R. Mattos, Xuemei Wan, Christopher C. Thornburg, Shinya Oishi, Kerry L. McPhail, Jane E. Ishmael, and Ville O. Paavilainen*



Cite This: *ACS Chem. Biol.* 2020, 15, 2125–2136



Read Online

ACCESS |



Metrics & More

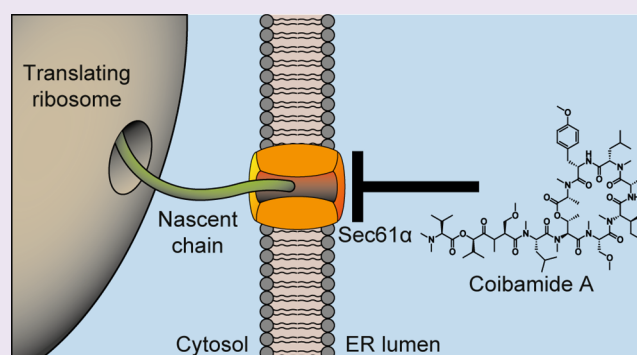


Article Recommendations



Supporting Information

ABSTRACT: Coibamide A (CbA) is a marine natural product with potent antiproliferative activity against human cancer cells and a unique selectivity profile. Despite promising antitumor activity, the mechanism of cytotoxicity and specific cellular target of CbA remain unknown. Here, we develop an optimized synthetic CbA photoaffinity probe (photo-CbA) and use it to demonstrate that CbA directly targets the Sec61 α subunit of the Sec61 protein translocon. CbA binding to Sec61 results in broad substrate-nonspecific inhibition of ER protein import and potent cytotoxicity against specific cancer cell lines. CbA targets a luminal cavity of Sec61 that is partially shared with known Sec61 inhibitors, yet profiling against resistance conferring Sec61 α mutations identified from human HCT116 cells suggests a distinct binding mode for CbA. Specifically, despite conferring strong resistance to all previously known Sec61 inhibitors, the Sec61 α mutant R66I remains sensitive to CbA. A further unbiased screen for Sec61 α resistance mutations identified the CbA-resistant mutation S71P, which confirms nonidentical binding sites for CbA and apratoxin A and supports the susceptibility of the Sec61 plug region for channel inhibition. Remarkably, CbA, apratoxin A, and ipomoeassin F do not display comparable patterns of potency and selectivity in the NCI60 panel of human cancer cell lines. Our work connecting CbA activity with selective prevention of secretory and membrane protein biogenesis by inhibition of Sec61 opens up possibilities for developing new Sec61 inhibitors with improved drug-like properties that are based on the coibamide pharmacophore.



INTRODUCTION

Natural products are a rich source of bioactive and specific chemical probes and serve as starting points for development of new therapeutics once their mechanism of action and cellular targets have been identified.^{1,2} Coibamide A (CbA)³ is an *N*-methyl-stabilized lariat depsipeptide (Figure 1) isolated from a *Caldora* species⁴ of marine cyanobacterium collected in Panama. CbA potently inhibits cell proliferation, migration, and invasive capacity, and in early assessments of the *in vivo* activity of the natural product, or simplified analogue, inhibited tumor growth in subcutaneous xenograft models of human glioblastoma and breast cancer.^{5,6} Further, CbA rapidly induces a macroautophagy stress response in mammalian cells, and a phase-specific G₁ cell-cycle block prior to cell death.^{5,7} The observed biological profile and distinct pattern of selectivity against cell lines of the National Cancer Institute (NCI) 60 human tumor cell line panel has generated considerable interest in CbA, resulting in development of total synthesis methods and revision of the absolute configuration of the natural product.^{8–10}

CbA inhibits expression of the integral membrane receptor, vascular endothelial growth factor receptor 2 (VEGFR-2), and its secreted ligand vascular endothelial growth factor A (VEGF-A). It induces mTOR-independent autophagy in a manner similar to apratoxin A (AprA), a previously characterized inhibitor of protein import into the early secretory pathway,⁵ despite yielding different cytotoxic profiles against cell lines of the NCI-60 tumor cell line panel.^{3,11} Protein secretion is a complicated multistep process¹² that begins when nascent secretory proteins are synthesized in the cytosol. Small molecule probes with a defined mechanism have allowed dissection of the basic function of the secretory pathway¹³ and provided new insights into the mechanism of protein transport into the endoplasmic reticulum.^{14–17} Such

Received: April 24, 2020

Accepted: July 1, 2020

Published: July 1, 2020



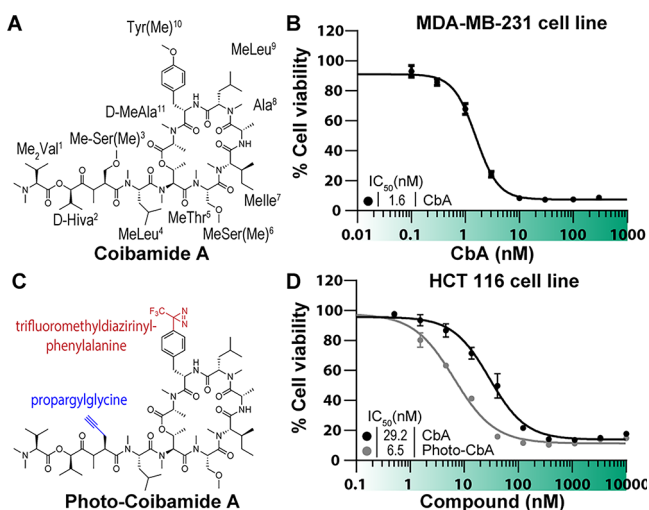


Figure 1. Cytotoxicity of synthetic and Pra-containing coibamides. (A) Structure of CbA. (B) Human MDA-MB-231 breast cancer cells were treated with increasing concentrations of synthetic CbA or vehicle (0.1% DMSO) and cell viability assessed at 72 h by an MTS end-point assay. (C) Structure of Photo-CbA. (D) Human HCT116 cells were treated with increasing concentrations of synthetic or photo-CbA in 0.1% DMSO, and cell viability assessed at 72 h by Alamar Blue assay.

probes can also serve as therapeutic lead scaffolds for targeting diseases where the secretory pathway plays a central role.¹⁸ The first step in protein secretion is entry into the endoplasmic reticulum (ER), after which newly synthesized secretory polypeptides undergo distinct maturation steps that enable correctly folded proteins to exit the ER and be targeted to their correct final destinations. Previously reported natural products that prevent protein entry into the secretory pathway include, in addition to AprA,¹⁴ HUN-7293 (pestatavin)^{19,20} and related synthetic cotransins,^{19–21} mycolactone A/B,^{15,22,23} decatransin,¹⁶ ipomoeassin F (IpoF),²⁴ and eeyarestatin I compounds.²⁵ However, the critical step inhibited by CbA during biogenesis of VEGFR-2 and VEGF-A and the direct cellular target of CbA remain unknown.

In the current study, we explore the structure–activity relationship (SAR) of CbA to develop an optimized CbA photoaffinity probe (photo-CbA), which allowed us to identify the Sec61 α subunit of the Sec61 protein translocation channel as the direct cellular binding target of CbA. Sec61 binding prevents cellular production of a broad range of secreted and integral membrane proteins that depend on Sec61 for their cotranslational biogenesis. The CbA binding site on Sec61 α near the luminal plug domain seems to be only partially overlapping to that of previously described substrate-nonselective Sec61 inhibitors AprA and mycolactone, suggesting

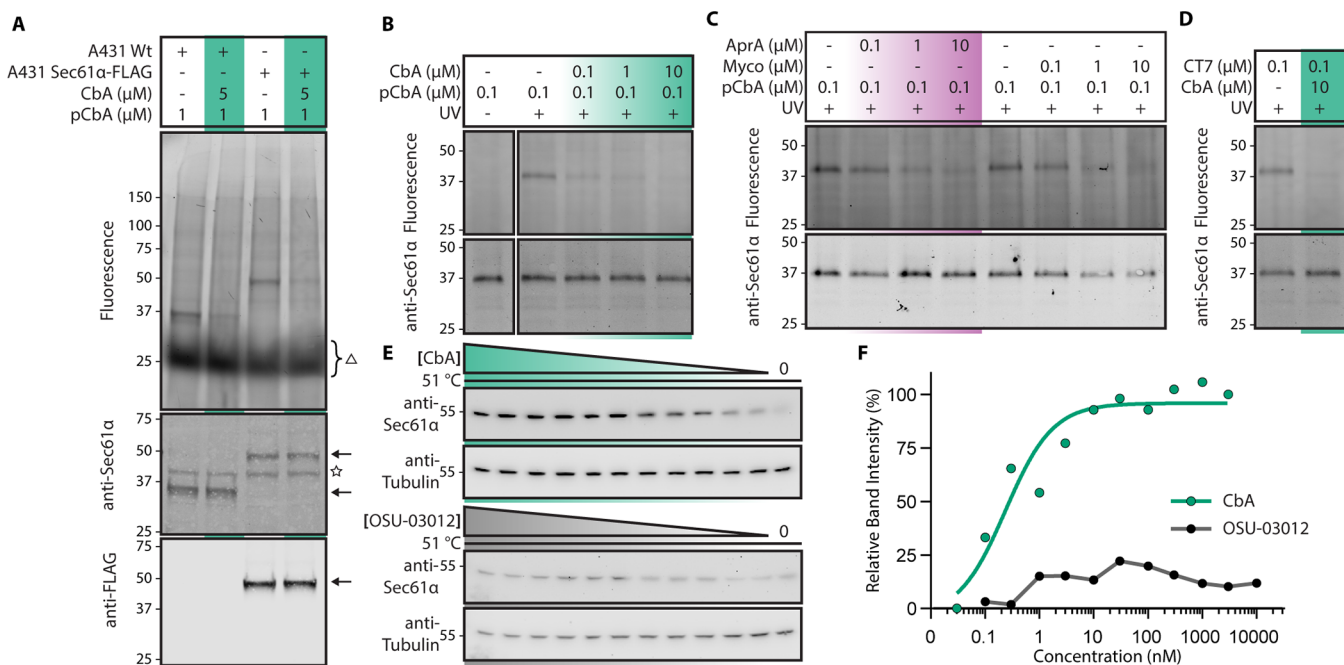


Figure 2. Photo-cross-linking of photo-CbA to Sec61 α and CbA stabilization of Sec61 in cells. Photocotransin (CT7) or photocoibamide (pCbA) cross-linking to cells or sheep rough microsomes (SRM). Samples were photolyzed and the covalent adduct detected by click-chemistry to TAMRA-azide reporter and in-gel fluorescence scanning and Western blotting. (A) A431 cell lines were first incubated with CbA or carrier, followed by incubation with photo-CbA, photolysis, and click chemistry. Following SDS PAGE, lysates were queried for in gel fluorescence and subsequently transferred for anti-Sec61 α and anti-FLAG Western Blot. Arrows indicate Sec61 (with or without a 10 kDa insert), star indicates nonspecific WB signal, triangle indicates free TAMRA dye within the gel. (B) As in A but in SRMs. Sample without UV irradiation shows the nonspecific background labeling of photo-CbA. (C) SRMs were first incubated with indicated concentrations of AprA, or Myco, followed by incubation with photo-CbA, photolysis, and click chemistry. (D) CT7 cross-linking to microsomes in the presence or absence of 10 μ M CbA. (E) Stabilization of intracellular Sec61 α by CbA. Isothermal concentration–response analysis of Sec61 α in the presence or absence of CbA (0.01 nM to 3 μ M), OSU-03012 (0.03 nM to 10 μ M), or 0.1% DMSO. Intact U87-MG glioblastoma cells were treated as indicated and subjected to heating at 51 $^{\circ}$ C for 3 min. Heat-treated cell suspensions were snap frozen, lysates cleared by centrifugation, and the soluble fraction analyzed by SDS-PAGE and Western blotting. Note that Sec61 α migrated above the 40 kDa molecular weight marker in several human cell lines using a standard Western blot protocol (Abcam ab183046; Figure S26C). (F) Quantification of immunoblot data shown in E. Sec61 α band intensity was normalized to tubulin, and data points were fitted using nonlinear regression analysis.

that CbA interacts with Sec61 through unique interactions. CbA also has differential growth inhibitory potential against a panel of cancer cells relative to AprA and IpoF.

RESULTS AND DISCUSSION

Synthesis of CbA and Its Photoaffinity Derivatization.

Obtaining sufficient quantities of CbA for detailed mechanism of action studies from field-collected material is highly challenging,³ and thus we first set out to establish a total synthesis for this *N*-methylated peptidic macrocycle (Figure 1A) using a modification of a previously reported method⁸ (see the Supporting Information). Briefly, we initially constructed the middle part of CbA (MeThr5–MeIle7: fragment 2) on (2-Cl)Trt resin by standard Fmoc-solid phase peptide synthesis, and then conjugated the *N*-terminal four residues (Me₂Val1–MeLeu4: fragment 1). After coupling of *D*-MeAla11 onto the Thr5 hydroxy group, the remaining sequence (Ala8–Tyr(Me)10: fragment 3) was appended. EDCI/HOAT-mediated cyclization of the open-chain precursor, which was obtained by cleavage from the resin by treatment with HFIP, afforded the expected CbA.⁸ Having a robust source of synthetic CbA, we proceeded with biological characterization of the synthetic product in human MDA-MB-231 triple negative breast cancer cells. These cells were previously identified as highly sensitive (IC₅₀ = 2.8 nM) to natural CbA,³ and we observed consistent cytotoxic potency (IC₅₀ = 1.6 nM) for the synthetic CbA (Figure 1B).

Similar to the previously reported photocotransin,²⁶ we aimed to install a diazirine group in CbA for photoactivated cross-linking to the binding target and an alkyne handle for *in situ* click chemistry coupling to fluorescent or affinity tags. All-*L*-CbA was reported to have moderate micromolar cytotoxicity against three cancer cell lines,²⁷ while [*D*-MeAla11]-all-*L*-CbA displayed high nanomolar activity against four cancer cell lines.⁹ Given the adverse effect of the *L*-MeAla11 configuration for CbA activity, we anticipated that the neighboring Tyr(Me)10 could be involved in target interactions and could be substituted with the nearly isosteric 4-[3-(trifluoromethyl)-3*H*-diazirin-3-yl]phenylalanine (Tdf) side chain. This substitution is further supported by the loss of activity for an AprA analogue in which the MeTyr is epimerized.²⁸

Positioning of the clickable alkyne amino acid was informed by a structure–activity relationship study to identify the optimal position for insertion of a propargylglycine (Pra) residue. In total, we synthesized six Pra/MePra-containing CbA analogues using the identical protocol with on-resin fragment condensation. Comparative antiproliferative testing in A549 lung cancer cells led to selection of residue position 3 for MePra in the targeted photoprobe (Figure S1). Dual modifications with MePra3 and Tdf10 afforded a potent photoaffinity probe, photocobamide (Photo-CbA) with an alkyne handle (IC₅₀ = 6.5 nM against HCT116 cells; Figure 1D).

Photo-CbA Directly Targets the Sec61 α Subunit of the Protein Translocon. To identify the direct photo-CbA photo-cross-linking partner in an unbiased manner, we incubated live human A431 carcinoma cells with photo-CbA either in the presence or in the absence of parent CbA, followed by photolysis in intact cells. Detection of photo-cross-linked adducts was then carried out following installation of a TAMRA fluorophore by Cu(I) catalyzed Click chemistry under denaturing conditions and in-gel fluorescence scanning. This revealed a single cross-linked band of approximately 37

kDa in molecular weight, which was efficiently competed by addition of excess unmodified CbA (Figure 2A, first 2 lanes). A prior observation that CbA prevents biogenesis and ER import of VEGFR-2 during or following protein translation⁵ suggests that CbA may target a component of the ER protein biogenesis machinery. The observed 37 kDa molecular weight corresponds to that of the Sec61 α subunit, which is the essential subunit of the protein translocon that forms the conduit through which newly synthesized proteins enter the secretory pathway.¹² As Sec61 α is the direct target of established highly selective natural products that inhibit ER import such as cotransins, AprA, decatransin, and mycolactone,²⁹ we speculated that CbA could prevent VEGFR-2 expression by directly inhibiting Sec61. Repeating the photo-cross-linking assay against cells in which the endogenous locus of Sec61 α has been edited to introduce additional sequence bearing a 3xFLAG epitope that increases the molecular weight by approximately 10 kDa revealed that the photo-cross-linked product shifted size accordingly (Figure 2A, last 2 lanes). As further validation that photo-CbA is cross-linking to Sec61 α , a nonglycosylated protein, we used endoglycosidase H treatment to strip glycans from proteins in our sample. While the abundant and glycosylated Sec61 translocon component, Translocation Associated Membrane Protein 1 (TRAM), shifted to a smaller molecular weight species, the photo-cross-linked product remained at approximately 37 kDa, indicating that the target of photo-CbA is a non glycosylated protein (Figure S26).

To compare the binding of photo-CbA to known inhibitors of Sec61 α , we then investigated cross-linking of photo-CbA and CT7, a potent and specific photoaffinity inhibitor of Sec61 α ,²⁶ in isolated ER microsomes. Incubation with photo-CbA yielded a single band of approximately 37 kDa apparent molecular weight as per the *in vivo* result, which could be competed out in a concentration dependent manner by the addition of excess unmodified CbA (Figure 2B). We then tested whether photo-CbA cross-linking can be competed with known Sec61 ligands, AprA or mycolactone.^{14,15,28} Both compounds prevented photo-CbA cross-linking in a concentration-dependent manner; similarly, addition of excess CbA competed for cross-linking by cotransin CT7, both consistent with the notion that the photo-CbA cross-linked adduct is with Sec61 α (Figure 2C and D).

We next used cellular thermal shift assays as an independent test of the ability of CbA to engage with Sec61 in cells. The feasibility of this approach was first interrogated by establishing a melting curve for Sec61 α by analysis of soluble protein fractions by Western blot following a heat challenge (Figure S26). For these studies, intact human U87-MG glioblastoma cells were subjected to temperatures ranging from 45 to 72 °C in the presence and absence of CbA, AprA, or an unrelated PDK-1 and putative immunoglobulin binding protein (BiP) inhibitor, OSU-03012. Both CbA and AprA stabilized Sec61 α , resulting in the continued detection of the presumed ligand-bound protein at a higher temperature range (60–66 °C) than for the relatively weak immunoreactivity observed for either vehicle- or OSU-03012-treated samples (Figure S26). On the basis of these results, a fixed temperature (51 °C) was then selected for isothermal dose–response fingerprinting of Sec61 α in the presence, or absence, of increasing concentrations of CbA (0.01 nM to 3 μ M) or OSU-03012 (0.03 nM to 10 μ M). Under these conditions, CbA stabilized Sec61 α in a concentration-dependent manner with half-maximal stabiliza-

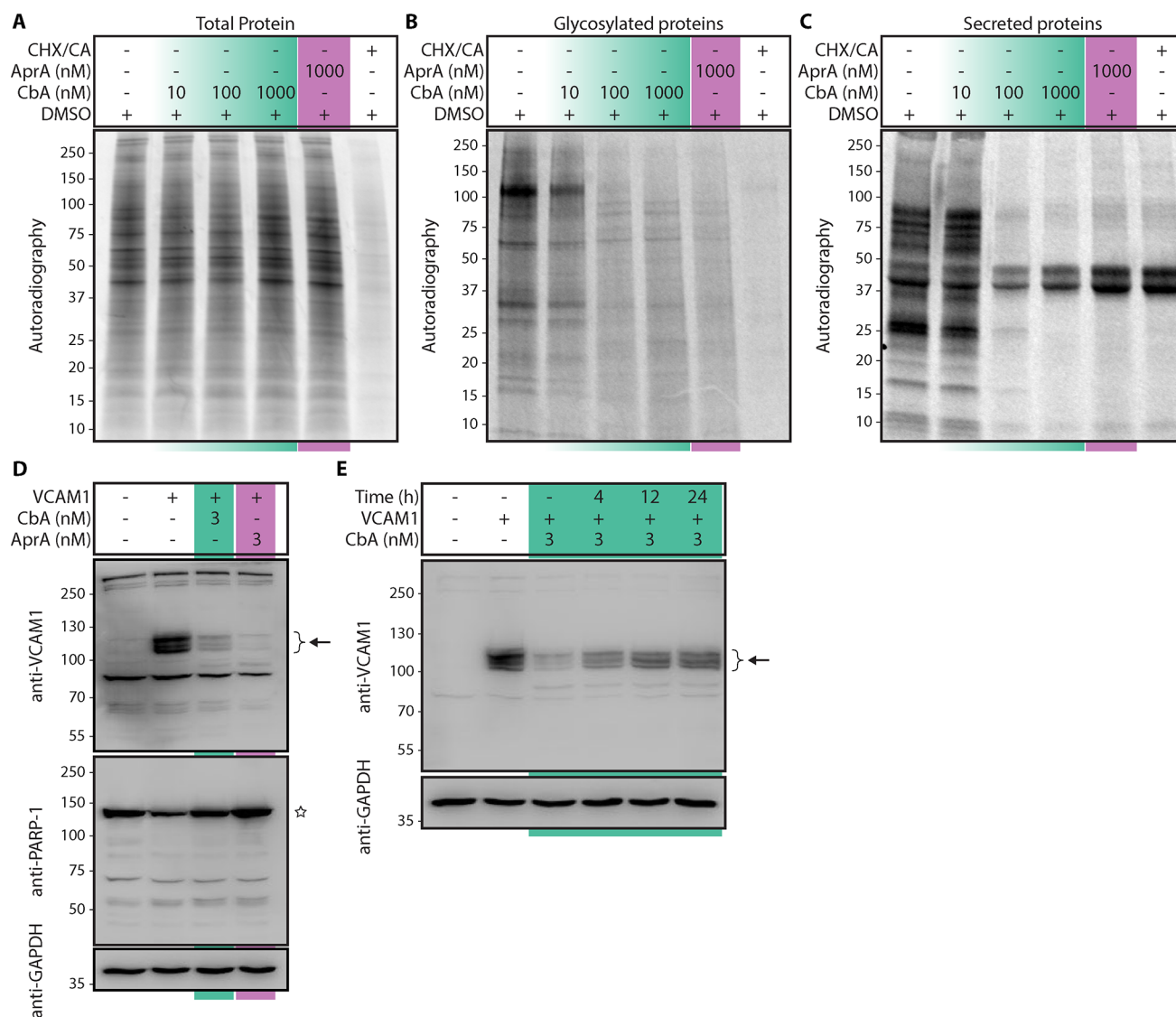


Figure 3. CbA specifically inhibits biogenesis of secretory and membrane proteins. (A to C) HCT-116 cells were labeled with ^{35}S -Met and ^{35}S -Cys in the presence of increasing concentrations of CbA. CHX/CA denotes control samples treated with cycloheximide and chloramphenicol to inhibit protein synthesis by cytosolic and mitochondrial ribosomes. Molecular weights are shown in kDa. (A) The collected cells were homogenized and analyzed by SDS-PAGE and autoradiography. (B) As in A but the samples are glycosylated protein fractions isolated with ConA-lectin affinity. (C) As in A but the samples are TCA-precipitated culture medium from the same experiment. (D) HEK-293T cells transiently expressing human VCAM1 were treated with 3 nM CbA, AprA, or vehicle (0.1% DMSO) at 5 h post-transfection and protein expression analyzed by Western Blotting at 24 h. (E) As in D, cells were treated with CbA (3 nM) or vehicle (0.1% DMSO) at 5 h post-transfection, incubated for a further 24 h, after which CbA was diluted 6-fold by the addition of fresh medium before the cells were harvested at the indicated time points. In D and E, the arrow indicates mature VCAM1 in several glycosylation states; the star denotes PARP-1.

tion observed at ~ 0.2 nM concentration, whereas no apparent stabilization of Sec61 α was observed with OSU-03012 (Figure 2E and F).

Collectively, these data provide robust evidence indicating that CbA directly and specifically interacts with the Sec61 α subunit of the ER protein translocation channel. All currently known natural product inhibitors of Sec61 bind at the same luminal Sec61 cavity,²⁹ and our photo-cross-linking data (Figure 2) suggests that also CbA binds Sec61 α at this or a partially overlapping region.

Coibamide Reversibly Inhibits Biogenesis of Secreted and Membrane Proteins. The Sec61 translocon facilitates a key step in protein maturation by mediating the insertion of substrate proteins into the ER membrane or across it into the luminal space.¹² To investigate the global impact of CbA on

cellular protein biogenesis, we performed metabolic labeling with ^{35}S -methionine/cysteine in HCT116 colon carcinoma cells and investigated the processing of newly synthesized proteins in the presence or absence of CbA. In these experiments, even micromolar CbA concentrations did not result in reduction of the production levels of total cellular proteins (Figure 3A). However, production of glycosylated and secreted proteins was severely inhibited by CbA in a concentration-dependent manner, and full inhibition was observed with 100 nM CbA (Figure 3B and C). Collectively, CbA treatment does not impact cellular protein synthesis but instead prevents cotranslational protein glycosylation and net nascent protein secretion, which both require function of the Sec61 translocon. In this experiment, the effect of CbA on nascent protein synthesis was similar to that of AprA, a

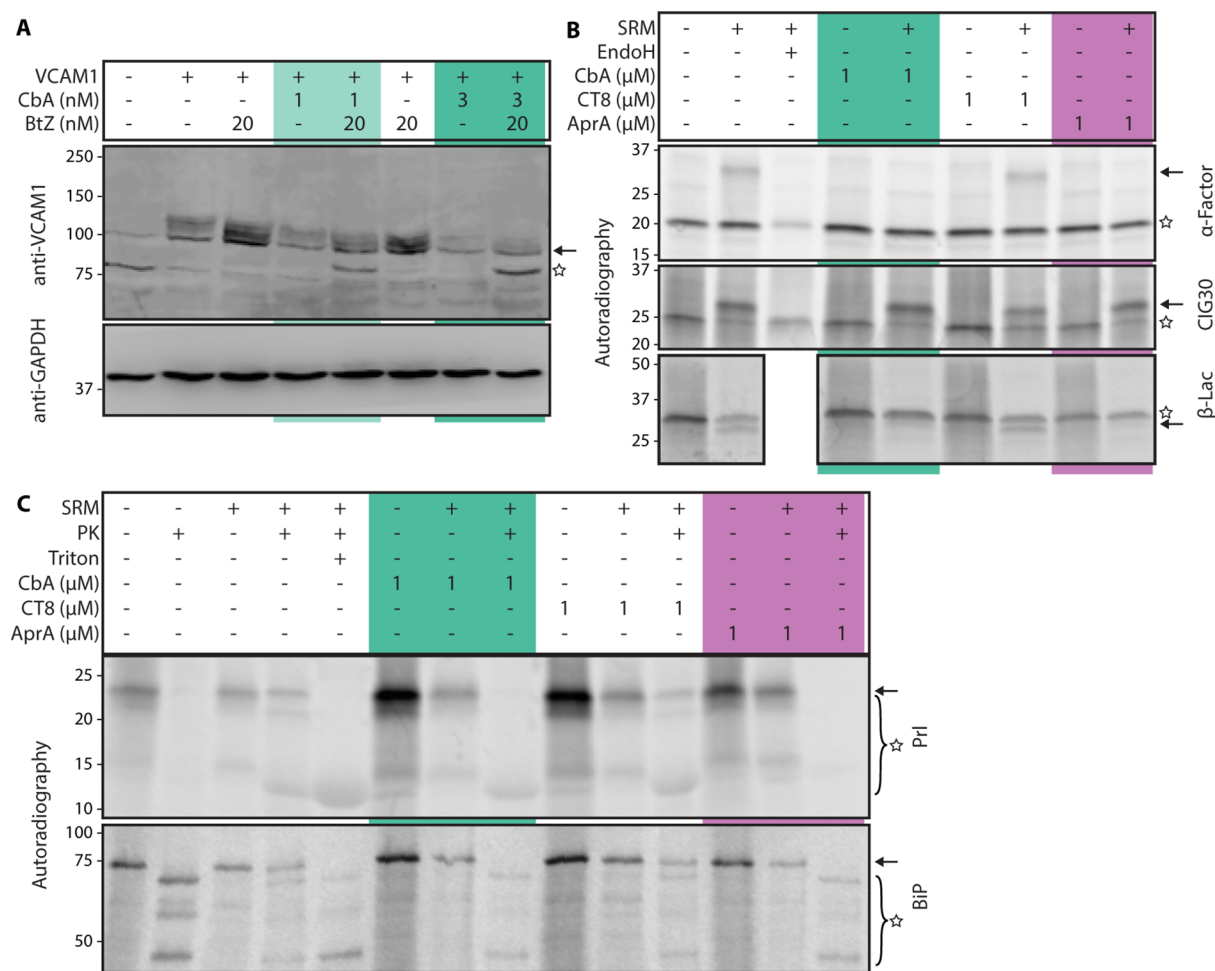


Figure 4. CbA inhibits translocation of a range of Sec61 substrates. (A and B) The star indicates the unprocessed form of the protein, and the arrow points to the processed, mature form. Molecular weights of the standards are shown in kDa. (A) Cells transiently expressing VCAM1 were treated 5 h post-transfection with either 1 or 3 nM CbA in the presence or absence of 20 nM proteasomal inhibitor bortezomib (BtZ). Whole cell lysates were analyzed by Western Blotting after 24 h. (B and C) For the *in vitro* translocation assay (IVT), the indicated proteins were translated in the presence of microsomes, 35 S-Met, and the indicated inhibitors. (B) Translocation of glycosylated proteins was assessed by change in migration in SDS-PAGE. Endoglycosidase treatment (EndoH) was used to demonstrate that the altered migration was due to glycosylation. Yeast α -factor, mouse elongation of very long chain fatty acids protein 3 (CIG30), beta-lactamase (β -Lac). (C) Translocation of nonglycosylated proteins was demonstrated by treatment with proteinase K (PK). The Hamster binding immunoglobulin protein (BiP) and bovine prolactin (PrI). The star indicates protein degradation products following PK digestion, and the arrow points to the intact protein.

previously described substrate-nonspecific inhibitor of ER protein translocation.¹⁴

We next set out to investigate the effects of CbA on the biogenesis of type I integral membrane proteins using human vascular cell adhesion molecule 1 (VCAM1) as a model protein. Biogenesis of this protein is potently inhibited by cotransin, a highly substrate-selective inhibitor of VCAM1 membrane insertion.^{19,20} We transiently expressed human VCAM1 in HEK293T cells and treated the cells with either CbA (3 nM), AprA (3 nM), or vehicle (0.1% DMSO) for 24 h. Immunoblot analysis of whole-cell lysates harvested after compound treatment revealed a strong reduction in VCAM1 expression in cells treated with either CbA or AprA (Figure 3D). Importantly, we did not observe evidence of proteolytic processing of poly[ADP-ribose] polymerase 1 (PARP-1), suggesting that caspase-dependent cell death is not involved in inhibition of VCAM1 expression. Further, dilution of CbA to subnanomolar concentrations, by the addition of fresh culture medium, resulted in a time-dependent reversal of VCAM1 expression inhibition, demonstrating that CbA

inhibits Sec61-mediated protein biogenesis in a reversible manner (Figure 3E).

Coibamide Inhibits Sec61-Mediated Translocation in a Substrate-Nonspecific Manner. Earlier studies have revealed that cotransin downregulates VCAM1 by preventing its Sec61-mediated ER insertion and causing the cytosolic displacement of the nascent VCAM1 polypeptide and subsequent cytosolic degradation by the ubiquitin proteasome system.²⁰ Thus, we set out to test whether CbA inhibits VCAM1 expression via a similar mechanism. Here, treating cells with CbA resulted in downregulation of VCAM1 expression, which was rescued in a time-dependent manner by treatment with bortezomib (BtZ), a specific inhibitor of the proteasome (Figure 4A). Therefore, CbA appears to inhibit VCAM1 expression during or after nascent VCAM1 synthesis, which could involve stages of ER targeting, membrane insertion, maturation, or protein trafficking. The observed accumulation of immature unglycosylated VCAM1 forms following CbA and BtZ treatment indicate that CbA interferes with proper VCAM1 maturation (Figure 4A).

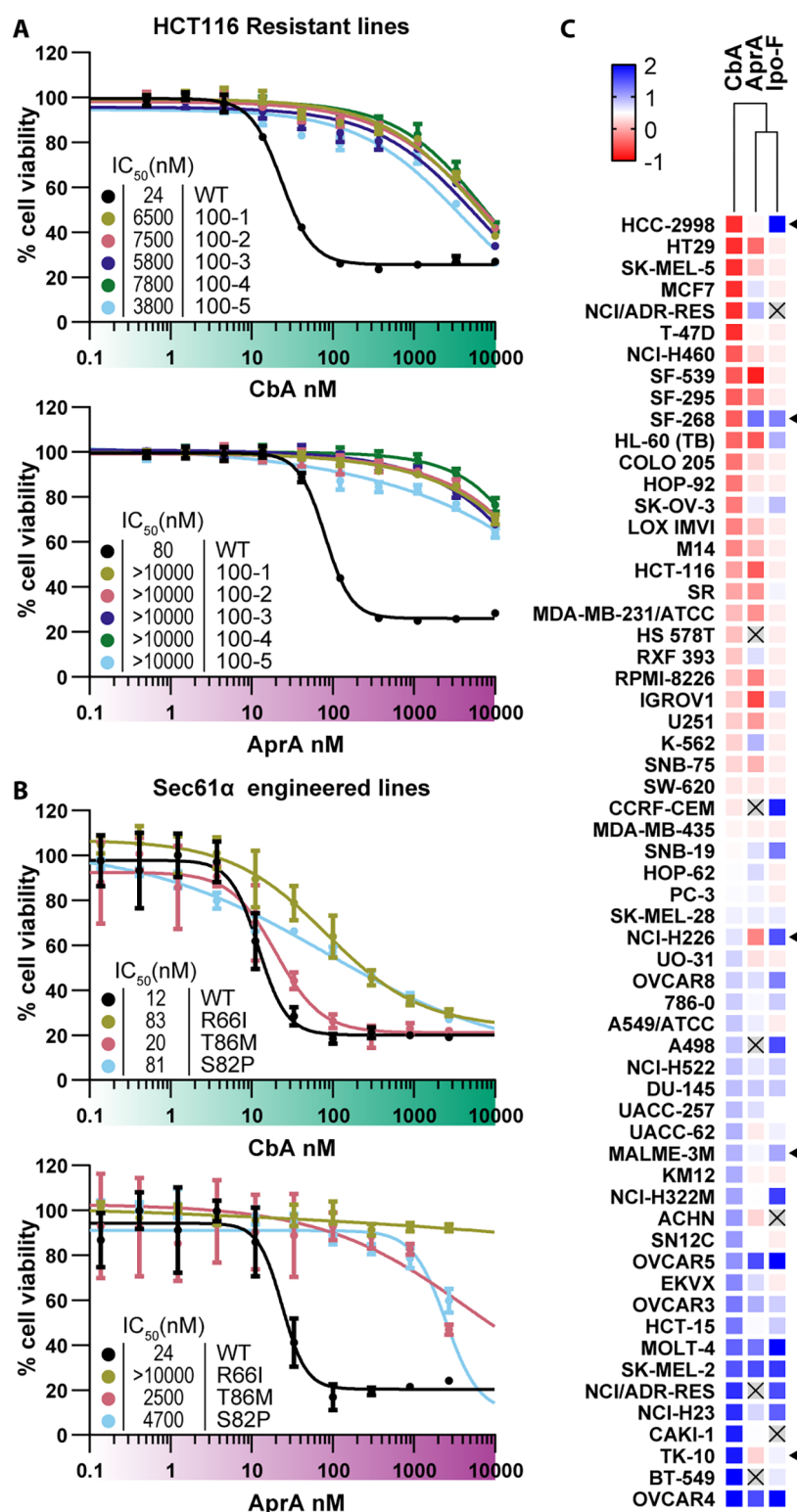


Figure 5. CbA mode of inhibition is specific compared to known Sec61 inhibitors. (A) Cell viability was measured by Alamar Blue assay (mean \pm SD, $n = 4$, all cell lines assayed simultaneously) for HCT-116 cell lines isolated on the basis of CbA resistance in the presence of concentration series of indicated compounds. (B) Cell viability was measured by Alamar Blue assay (mean \pm SD, $n = 4$, all cell lines assayed simultaneously) for HEK293FRT cells stably expressing Sec61 α mutants in the presence of concentration series of indicated compounds. (C) Comparison of published NCI60 data for CbA,³ AprA,¹¹ and IpoF.³³ The heat map was derived by plotting each GI₅₀ value divided by the median GI₅₀ for that compound. X indicates a cell line that was not tested. Closed arrowhead indicates cell lines with most notable differences across the three compounds.

To dissect the biochemical mechanism by which CbA prevents maturation of nascent secretory proteins, we used a reconstituted mammalian translation system supplemented

with isolated sheep rough microsomes (SRM).³⁰ In these experiments, CbA did not influence protein translation of any of the diverse Sec61 substrate proteins tested, which included

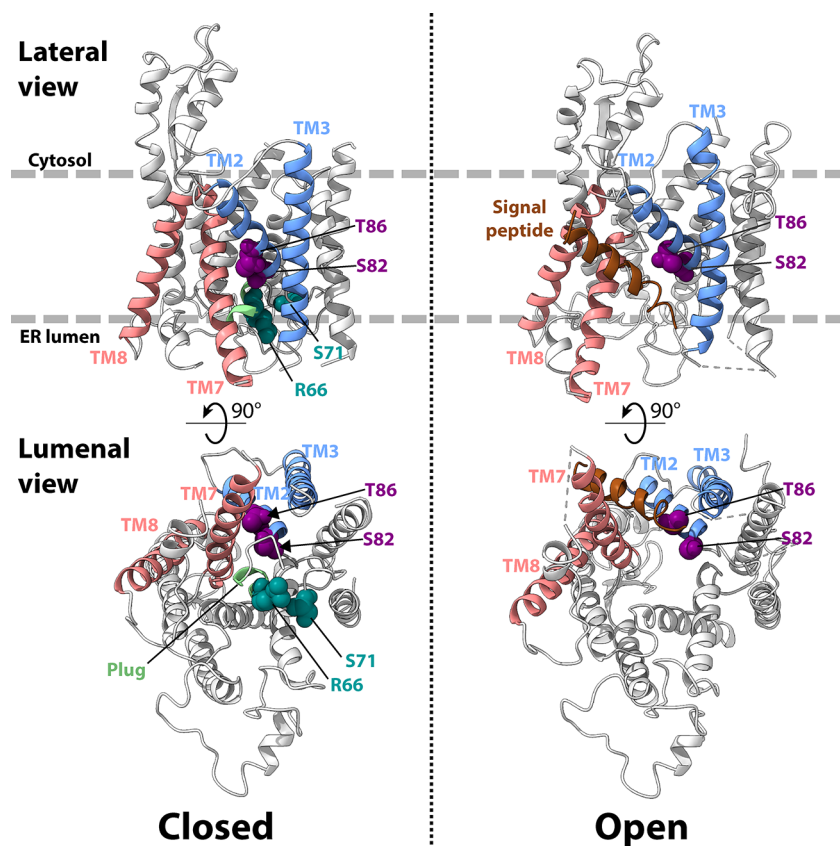


Figure 6. Structure of Sec61 complex and location of resistance point mutations. Lateral and ER luminal views in closed and open conformations of the Sec61 complex are shown. Lateral gate helices 2 + 3 (light blue) and 7 + 8 (light coral) as well as the plug region (light green) are indicated on the Sec61 α core subunit (light gray). Mutations in Sec61 α at residues 82 and 86 in helix 2 are shown in purple, luminal plug residues 66 and 71 are shown in teal. The open but stalled Sec61 complex is shown with bound preprolactin signal sequence (brown). Structural coordinates were obtained from the Protein Data Bank, IDs 3J7Q and 3JC2.

secreted proteins (yeast α -factor, β -lactamase, BiP, preprolactin) and a polytopic membrane protein (CIG30). We assayed the inhibitory effect of CbA on protein processing *in vitro* and compared the effects with those of AprA and cotransin analogue CT8 (Figure 4 B). CbA prevents both glycosylation (yeast α -factor) and signal peptide cleavage (β -lactamase). Processing of secreted proteins was inhibited, while CIG30, a multipass membrane protein, was resistant against CbA and all other translocation inhibitors tested (CT8, AprA) and is also known to be resistant toward mycolactone,¹⁵ consistent with the critical CIG30 dependence for the ER membrane protein complex (EMC) instead of Sec61 for its biogenesis.³¹

To further investigate the CbA-sensitive stage of protein translocation, we again used the reconstituted *in vitro* translation and translocation system and queried the accessibility of Sec61 substrate proteins to exogenous proteinase K (PK) in the presence or absence of SRM. In these reactions, nascent polypeptides of ER translocated BiP and preprolactin (PrI) are shielded from protease digestion in the presence of SRM, yet are cleaved in the absence of SRM or when microsomes are solubilized with detergent indicative of membrane translocation (Figure 4C). However, the addition of 1 μ M CbA, CT8, or AprA into SRM-containing reactions renders the nascent polypeptides sensitive to PK (Figure 4C), indicating that these compounds prevent ER entry of the newly synthesized proteins. Collectively, our data (Figures 3D, 4) indicate that CbA potentially prevents ER insertion and

subsequent processing of a wide range of secreted and integral membrane proteins with the notable exception of membrane proteins with N-terminal transmembrane segments of the type III topology.

Coibamide Binding to Sec61 Is Distinct from Other Translocation Inhibitors. In an effort to map the location of the CbA binding site on Sec61 α , we used a genetic selection approach in mammalian cells and attempted to identify specific resistance-conferring point mutations. Such chemogenetic screens are a powerful means to discover novel mutations and mechanisms of action for cell-active small molecules and have been used to identify point mutations in SEC61A1 that confer specific resistance to cytotoxicity of different Sec61 inhibitors.^{14,16,17,32} We exposed EMS mutagenized HCT116 colon carcinoma cells to 50–100 nM CbA ($IC_{50} \sim 29$ nM), which resulted in a majority of the cells dying, yet during selection, six colonies grew and were isolated. Monoclonal cell lines derived from the colonies exhibited strong resistance to CbA (up to 100-fold desensitization) and to an even greater degree to AprA (Figure 5A). Sequencing the coding regions of the SEC61A1 gene revealed a single nucleotide transition encoding for the heterozygous Sec61 α mutation S71P. In contrast to CbA selection, previous unbiased resistance mapping screens in HCT116 cells with cotransin, AprA, and dextranin all revealed a range of Sec61 α mutations conferring specific resistance to the tested Sec61 inhibitors. To assay the effect of previously identified Sec61 α mutations, we tested a panel of mutations in naive HEK293 FRT cells where the

mutant Sec61 α proteins are stably expressed from an exogenous locus at a similar level as endogenous Sec61 α .¹⁷ As we reported earlier, all of the tested mutations conferred strong resistance to AprA,¹⁴ but only moderate resistance was observed for CbA (Figure 5B). This finding is surprising especially for the R66I mutation that confers essentially complete resistance for all known Sec61 inhibitors,^{14–16,24} yet only causes moderate (~7-fold) desensitization to CbA (Figure 5B). The Sec61 α mutations S82P and T86M that confer resistance to other Sec61 inhibitors, but not CbA, are clustered on the luminal end of the Sec61 lateral gate, whereas mutations R66I and S71P are located in different parts of the Sec61 plug domain (Figure 6). Taken together, these mutational results suggest that CbA may interact with Sec61 in a unique manner or possibly bind a different conformation of the channel.

SUMMARY

Here, we report the comprehensive identification of target interactions of coibamide A (CbA), a cytotoxic marine natural product, with the ability to inhibit biogenesis of secreted and integral membrane proteins. By developing an isosteric photoaffinity probe of CbA, we demonstrate that the main binding target of CbA in mammalian cells is the Sec61 α subunit of the Sec61 protein translocon complex. Metabolic labeling experiments in cells and biochemical ER translocation experiments indicate that CbA inhibits cotranslational Sec61-facilitated ER translocation in a substrate-nonspecific manner. Finally, through an unbiased mutational mapping approach, we demonstrate that the cytotoxic potential of CbA for mammalian cells results from Sec61 inhibition, likely through binding of a Sec61 site partially overlapping with other substrate-selective and nonselective Sec61 inhibitors.

The Sec61 translocon forms a membrane channel which facilitates the essential ER membrane translocation or membrane integration step during biogenesis of secretory or integral membrane proteins, respectively. As rapidly proliferating cancer cells display heightened dependence on protein synthesis, pharmacological targeting of cellular proteostatic pathways, including the ER protein biogenesis machinery, has potential for the development of new therapeutic strategies,³⁴ prompting an interest in finding new privileged scaffolds to target critical proteostasis factors. Recent work has identified many structurally distinct natural product small molecules that appear to have evolved independently in distinct microorganisms to target Sec61 as a way to modulate or prevent biogenesis of secreted or integral membrane proteins. Intriguingly, all of these inhibitors appear to target Sec61 at its luminal cavity near the Sec61 lateral gate and plug domains (Figure 6) whether they inhibit production of Sec61 substrate proteins in a substrate-selective (cotransins)^{19,20} or substrate-nonspecific (AprA, mycolactone, IpoF, decatransin)^{14–16,22,24} manner.

The luminal Sec61 cavity where all reported inhibitors bind has been outlined by mutations identified in several independent studies in both mammalian and yeast chemogenomic screens (reviewed in ref 29). Together the mutations outline a general binding pocket at the luminal end of the Sec61 α subunit, which appears to be at least partially shared by all five published inhibitors. Yet, a distinct pattern of resistance has been observed for some of these inhibitors,^{14,24} suggesting that despite occupying the same general binding cavity, they utilize different specific interactions with Sec61 or bind

different conformations of the inherently dynamic channel. Specifically, Sec61 α mutations R66I and S82P confer potent resistance to all other known Sec61 inhibitors, while only conferring mild resistance to CbA. This suggests that CbA may bind Sec61 in a unique way, possibly by targeting a conformation in which the plug has moved to a different position. This notion is also supported by failure of our unbiased screen to identify common Sec61 α mutations, which have been identified for several inhibitors earlier in multiple resistance mutation screens.^{14,16,17,24} Future structural studies will be required to definitively characterize the binding modes of Coibamide A and other Sec61 inhibitors and can provide a basis for understanding means for inhibiting Sec61 in a substrate-selective manner.

This study and earlier work reveal an expansion of the binding site for Sec61 inhibition by diverse natural and synthetic inhibitors and prompt the question whether the observed binding differences translate to different cellular phenotypes. So far only two inhibitor classes, cotransins and CADA, have been reported to inhibit biogenesis of Sec61 client proteins with substrate selectivity. All the other reported natural product inhibitors prevent biogenesis of nearly all Sec61 dependent secreted and membrane proteins. Preventing synthesis of key proteins required for cancer cell survival and proliferation forms the basis for targeting cancer cells with substrate-selective Sec61 inhibitors.^{29,36}

Also, the substrate-nonspecific inhibitors AprA and coibamide A have demonstrated a therapeutic possibility to target cancer cells in *in vivo* models of human cancer,^{5,28,33,37} albeit with a limited therapeutic window. It remains unclear how structurally different Sec61 inhibitors with a seemingly identical biochemical inhibition mechanism could be leveraged for the design of cell type selective therapeutic lead scaffolds. To investigate this, we examined the published comparative growth inhibitory phenotypes across the cell lines assayed in the USA National Cancer Institute panel of 60 cancer cell lines (NCI-60)³⁸ against CbA,³ AprA,¹¹ and IpoF.³⁹ This correlative analysis revealed that each of the three compounds was designated as “COMPARE-negative,” suggestive of having distinct cytotoxic mechanisms. While not all data from the two testing events for each compound were available, there were activity data from one test event for at least 55 cell lines in each case, out of a total of 61 different cell lines tested across the three compounds. Because all three compounds appear to cause cytotoxicity by targeting the same site on Sec61 in a substrate-nonspecific manner, it is remarkable that the NCI-60 panel fails to recognize them as a mechanistic set. Comparison of the relative sensitivities of the tested cell lines reveals notable examples of differential cell targeting despite a lack of common trends at the level of histological cell types (Figure 5C). For example, the SF268 CNS cancer cell line ranks in the top 10 most sensitive to CbA (GI₅₀ 1.5 nM), yet it is in the 10 least sensitive cell lines to AprA (GI₅₀ 51 nM) and is also less sensitive to IpoF (GI₅₀ 120 nM). Further, HCC-2998 colon cancer cells are highly sensitive to CbA (GI₅₀ < 1 nM) and AprA (GI₅₀ 3.7 nM), yet they are one of the most resistant of the cell lines exposed to IpoF (GI₅₀ > 1000 nM). Finally, the renal cell line TK-10 appears to be much more sensitive to AprA and IpoF over CbA. Collectively, the NCI-60 profiling data reveal surprising cell type selectivity for these three compounds that induce cytotoxicity through binding and global inhibition of ER protein import. Possible explanations for the observed differences in cell type specificities include

differences in compound bioavailability, differential cell export by diverse multidrug efflux pumps, and differences in the cellular Sec61 inhibition mechanism by the ability to, for example, target specific Sec61 cofactor complexes. Together, these findings support the notion that structurally distinct Sec61 binding inhibitors could be developed to target specific diseased cells and tissues. In support of this notion, changes in the structure of AprA and CbA have yielded compound variants with reduced general cytotoxicity, while retaining efficacy in human tumor xenograft models.^{7,33,40} Further, modifications to the structure of mycolactone demonstrated that its cytotoxic and anti-inflammatory effects can at least partially be dissociated from each other.⁴¹ Finally, modifications to the side-chains of the substrate-selective Sec61 inhibitor cotransin altered the range of inhibited Sec61 substrates.²¹

Taken together, our work adds the structurally distinct cyclic peptide CbA to the class of potent Sec61 inhibitors whose on-target interactions at the Sec61 α lateral plug region prevent biogenesis of secreted protein factors and integral membrane proteins. Our work expands the class of structurally unique chemotypes that inhibit Sec61 and permit targeting of distinct cell types, which could be particularly relevant in diseases such as cancer, inflammation, and certain viral diseases, where Sec61-facilitated protein biogenesis contributes to disease progression. Finally, convergent evolution that resulted in the appearance of multiple classes of inhibitors presumably targeting diverse eukaryotic Sec61 channel orthologs highlights the important role that modulating protein biogenesis of extracellular proteins has for diverse microbial cells in distinct ecological niches.

METHODS

General Method for Synthetic Coibamide Compounds. ¹H NMR spectra were recorded using a JEOL ECA-500 spectrometer. Chemical shifts are reported in δ (ppm) relative to Me₄Si (in CDCl₃) as an internal standard. ¹³C NMR spectra were recorded using a JEOL ECA-500 spectrometer and referenced to the residual solvent signal (δ 77.00 ppm). High resolution mass spectra (HRMS) were recorded on a Shimadzu LC-ESI-IT-TOF-MS instrument. Optical rotations were measured using a JASCO P-1020 polarimeter. For flash chromatography, Wakogel C-200E (Wako) was employed. For analytical HPLC, a Cosmosil 5C18-ARII column (4.6 \times 250 mm, Nacalai Tesque, Inc.) was employed with a linear gradient of CH₃CN (with 0.1% (v/v) TFA) in H₂O at a flow rate of 1 mL/min, and eluting products were detected by UV at 220 nm. Preparative HPLC was performed using a Cosmosil 5C18-ARII preparative column (20 \times 250 mm, Nacalai Tesque, Inc.) at a flow rate of 8 mL/min.

Reagents for Chemical Biology. The production and purification of translocation inhibitors have been described previously: CT7 and CT8,²⁶ AprA,⁴² and mycolactone.¹⁵ OSU-03012 (AR12) was purchased from Millipore-Sigma. Sheep rough microsomes were isolated as previously described.⁴³

DNA Constructs and Transfections. DNA constructs encoding *in vitro* transcription templates for the cell-free translocation assays were PCR amplified using 5'-primers containing either T7 or SP6 promoter, a Kozak sequence, and a region complementary to the 5'-end of the gene. The 3'-primers contained a stop-codon and a region complementary to the 3'-end of the gene. For analysis of VCAM1 expression, full length VCAM1 in pCDNA3.1²⁰ was transiently expressed in HEK293T cells using jetPRIME Transfection Reagent (Polyplus transfection) 5 h before treatment.

SDS-PAGE, Autoradiography, and Western Blot. SDS-PAGE was performed either with Tris/Tricine or with TGX stain-free polyacrylamide gels (Bio-Rad). For autoradiography, the dried gels were exposed to a storage phosphor screen (GE Healthcare) and

imaged on a Typhoon phosphorimager (GE Healthcare). For Western blotting, proteins were transferred to nitrocellulose membranes (Bio-Rad). Following blocking of the membranes with Odyssey Blocking Buffer (PBS; LI-COR Biosciences) or 5% (w/v) nonfat dry milk in 50 mM Tris-HCl, pH 7.4, 150 mM NaCl (TBS) plus 0.1% Tween-20 (TBS-Tween), the membranes were first incubated with the appropriate primary antibodies and then with the appropriate secondary antibodies and finally imaged on an Odyssey infrared fluorescent scanner (LI-COR Biosciences) or a MyECL image analysis system (Thermo Fisher Scientific). All antibodies were from commercial sources and used according to the recommendations of the manufacturer.

Cell-Free Translation/Translocation Assays. *In vitro* transcription, translation, and translocation assays were done as previously described.^{14,30} The indicated genes were transcribed with T7 or SP6 polymerase, translated at 32 °C in the presence of microsomes, ³⁵S-Met, and indicated inhibitors. The translocation was confirmed either with endoglycosidase (EndoH) treatment or protease protection assay with proteinase K (PK). All the samples were TCA-precipitated before gel analysis. The synthesized proteins were detected by SDS-PAGE and autoradiography.

Photoaffinity Labeling. The photoaffinity labeling and click chemistry with microsomes were done as previously described.¹⁷ Sheep rough microsomes (SRMs) containing 100 nM Sec61 were first incubated for 30 min with indicated inhibitors, then with 100 nM photocoibamide or photocotransin CT7 for 10 min and cross-linking performed by UV-irradiation for 10 min. After denaturation with SDS, copper catalyzed Click chemistry was used to label the cross-linked adducts with the fluorescent group. The labeled proteins were analyzed by SDS-PAGE and in-gel fluorescence. For in cell photo-cross-linking, 1.5 \times 10⁵ A431 cells were plated into each well on a 12-well plate and grown for 24 h. After washing the cells twice with Dulbecco's PBS, media containing either the competing, unlabeled CbA, or vehicle (0.1% DMSO) were added. The cells were incubated in the cell incubator for 1 h, photo-CbA added, and the incubation continued for 30 min. The wells were washed twice with Dulbecco's PBS and photolyzed with UV irradiation (50 W, 365 nm) for 10 min. Cells were collected by scraping, pelleted, and resuspended into 50 mM HEPES, pH 7.5, 100 mM KOAc, 250 mM sucrose, 2 mM Mg(OAc)₂, 1% Triton X-100, and protease inhibitor (Pierce Protease Inhibitor, EDTA-free). The lysed cells were centrifuged at 21 100g for 10 min, the supernatant collected, and the proteins denatured by adding 1.1% SDS. The click chemistry and gel analysis were done as with the reactions containing SRMs.

Cell Culture and Cell Viability Assays, Pulse-Labeling of Cells. A431, HEK293T, and HEK293FRT cells were cultured in DMEM supplemented with 10% FBS. HCT-116 cells were cultured in McCoy's 5A media supplemented with 10% FBS. U87-MG cells were cultured in Minimum Essential Media (MEM) with 10% FBS, L-glutamine (2 mM), and 1% penicillin and streptomycin. MDA-MB-231 cells were cultured in MEM with Earl's salts plus 1% penicillin/streptomycin and 10% FBS. All cell lines were incubated at 37 °C under 5% CO₂. The activity of synthetic coibamide and photoaffinity analogues was tested in MDA-MB-231 and A549 cells after 72 h by MTS assay. All other cell viability assays were performed by seeding PerkinElmer Viewplate-96 plates at a density of 2.5 \times 10³ cells per well. Cells were allowed 24 h to adhere and then treated with indicated concentrations of inhibitors or vehicle (0.1% DMSO) for a further 72 h. Viability was estimated by the addition of Alamar Blue (Life Technologies) and measuring fluorescence after a further 4 h. Pulse-labeling experiments were performed by seeding six-well plates with 5 \times 10⁵ cells per well and allowing 24 h for cells to adhere. Cells were washed twice with PBS, then exchanged into Met-Cys free media with indicated concentrations of inhibitors for 30 min. 100 μ Ci of PerkinElmer EXPRE³⁵S³⁵S Protein Labeling Mix was then added per well. Media were collected, and the cells were harvested by scraping them into ice cold PBS after 30 min. Total protein was acquired by RIPA extraction from the cell pellet. Glycosylated protein was acquired by Concanavalin A purification, and secreted protein was acquired by TCA precipitation of the media.

Cellular Thermal Shift Assay. Assays were carried out according to a method previously described by Jafari and co-workers.⁴⁴ Briefly, a melting curve for Sec61 α was established in U87-MG glioblastoma cells. Whole cells were treated as indicated for 1 h, harvested using trypsin, and collected by gentle centrifugation at 300g for 3 min. Cell pellets were resuspended in PBS supplemented with PMSF and benzamidine to a final cell density of $\sim 2 \times 10^6$ cells/mL. The resulting cell suspension was equally distributed into PCR tubes and subjected to a range of temperatures (45 to 72 °C) using a Veriti 96-well thermal cycler. Cells were heated to the designated temperature for 3 min and immediately snap-frozen in liquid nitrogen. All samples were subjected to two freeze–thaw cycles. Lysates were cleared by centrifugation at 18,000g for 20 min, at 4 °C, and the supernatants were carefully transferred to new tubes for immunoblot analysis. For isothermal concentration–response fingerprinting of Sec61 α , U87-MG cells were harvested, as above, and resuspended in fresh medium to a cell density of $\sim 4 \times 10^7$ cells/mL. CbA, OSU-03012, or DMSO (final 0.1%) in 50 μ L of cell medium was added to 15 μ L of the cell suspension and incubated at 37 °C for 30 min. Cells were then subjected to a 51 °C heat treatment in a Veriti 96-well thermal cycler for 3 min and immediately snap-frozen in liquid nitrogen. The samples went through two freeze–thaw cycles, centrifugation, and preparation for immunoblot analysis as described above.

Resistant Cell Line Isolation. For obtaining resistant cell lines, HCT-116 cells were mutagenized by incubation with ethylmethanesulfonate (EMS) at a concentration of 2000 μ g/mL for 60 min. Cells were allowed 48 h to recover, then cultured in the presence of 50–100 nM coibamide A for 14 days, after which cell colonies were isolated by disc cloning and cultured further in drug-free media. Total RNA was isolated using Trizol reagent according to the manufacturer's instructions. Total cDNA was synthesized using anchored oligo(dT) primers and SuperScript IV reverse transcriptase (Invitrogen). Different cDNAs were amplified with Phusion polymerase (Thermo Fisher Scientific) and sequenced bidirectionally by Sanger sequencing.

■ ASSOCIATED CONTENT

SI Supporting Information

The Supporting Information is available free of charge at <https://pubs.acs.org/doi/10.1021/acscchembio.0c00325>.

Supporting methods, compound characterization data (Figures S1–S25), and supplemental biological experiment data (Figure S26 and Tables S1 and S2) (PDF)

■ AUTHOR INFORMATION

Corresponding Author

Ville O. Paavilainen – Institute of Biotechnology, University of Helsinki, Helsinki 00014, Finland; orcid.org/0000-0002-3160-7767; Phone: +358-50-448 4600; Email: ville.paavilainen@helsinki.fi

Authors

Dale Tranter – Institute of Biotechnology, University of Helsinki, Helsinki 00014, Finland; orcid.org/0000-0001-7757-5484

Anja O. Paatero – Institute of Biotechnology, University of Helsinki, Helsinki 00014, Finland; orcid.org/0000-0003-2193-2483

Shinsaku Kawaguchi – Graduate School of Pharmaceutical Sciences, Kyoto University, Kyoto 606-8501, Japan

Soheila Kazemi – Department of Pharmaceutical Sciences, College of Pharmacy, Oregon State University, Corvallis, Oregon 97331, United States

Jeffrey D. Serrill – Department of Pharmaceutical Sciences, College of Pharmacy, Oregon State University, Corvallis, Oregon 97331, United States

Juho Kelloso – Institute of Biotechnology, University of Helsinki, Helsinki 00014, Finland

Walter K. Vogel – Department of Pharmaceutical Sciences, College of Pharmacy, Oregon State University, Corvallis, Oregon 97331, United States

Uwe Richter – Molecular and Integrative Biosciences Research Programme, Faculty of Biological and Environmental Sciences, University of Helsinki, Helsinki 00014, Finland

Daphne R. Mattos – Department of Pharmaceutical Sciences, College of Pharmacy, Oregon State University, Corvallis, Oregon 97331, United States

Xuemei Wan – Department of Pharmaceutical Sciences, College of Pharmacy, Oregon State University, Corvallis, Oregon 97331, United States

Christopher C. Thornburg – Frederick National Laboratory for Cancer Research, Leidos Biomedical Research, Inc., Frederick, Maryland 21702, United States; orcid.org/0000-0002-4657-6895

Complete contact information is available at: <https://pubs.acs.org/doi/10.1021/acscchembio.0c00325>

Author Contributions

A.O.P., D.T., J.E.I., U.R., and V.O.P. designed the chemical biological and pharmacological experiments. S.K. and S.O. designed and synthesized the CbA probes. A.O.P., D.T., J.K., S.Kaw., S.Kaz., T.M., M.N., S.K., S.O., J.D.S., D.R.M., X.W., and V.O.P. conducted the experiments. A.O.P., D.T., J.E.I., K.L.M., S.O., V.O.P., C.C.T., and W.K.V. analyzed and interpreted the data. A.O.P., D.T., J.E.I., K.L.M., S.O., and V.O.P. drafted or revised the article.

Author Contributions

[#]These authors contributed equally

Notes

The authors declare no competing financial interest.

■ ACKNOWLEDGMENTS

This work was supported by the Academy of Finland (grants 289737 and 314672 to V.O.P., 299762 to J.K.) and Sigrid Juselius Foundation (V.O.P.), and in part by a Discovery Grant from the American Brain Tumor Association (J.E.I.); NIH Fogarty International Center ICBG grant TW006634-06 (K.L.M.); NIGMS R01GM132649 (J.E.I., K.L.M., S.O., V.O.P.); NCCIH T32AT010131 (D.R.M.); JSPS KAKENHI (24659004); AMED (JP17a m 0101092j0001; JP18lm0203006j0002); Takeda Science Foundation. The slaughterhouse Vainion Teurastamo is acknowledged for providing the sheep pancreas for isolating the microsomes. We are grateful to T. Matsuda and T. Kitamura (Kyoto University) for their technical assistance.

■ REFERENCES

- (1) Newman, D. J., and Cragg, G. M. (2016) Natural Products as Sources of New Drugs from 1981 to 2014. *J. Nat. Prod.* 79, 629–661.
- (2) Carlson, E. E. (2010) Natural products as chemical probes. *ACS Chem. Biol.* 5, 639–653.
- (3) Medina, R. A., Goeger, D. E., Hills, P., Mooberry, S. L., Huang, N., Romero, L. I., Ortega-Barría, E., Gerwick, W. H., and McPhail, K. L. (2008) Coibamide A, a potent antiproliferative cyclic depsipeptide from the Panamanian marine cyanobacterium *Leptolyngbya* sp. *J. Am. Chem. Soc.* 130, 6324–6325.
- (4) Engene, N., Paul, V. J., Byrum, T., Gerwick, W. H., Thor, A., and Ellisman, M. H. (2013) Five chemically rich species of tropical marine

- cyanobacteria of the genus *Okeania* gen. nov. (Oscillatoriales, Cyanoprokaryota). *J. Phycol.* 49, 1095–1106.
- (5) Serrill, J. D., Wan, X., Hau, A. M., Jang, H. S., Coleman, D. J., Indra, A. K., Alani, A. W. G., McPhail, K. L., and Ishmael, J. E. (2016) Coibamide A, a natural lariat depsipeptide, inhibits VEGFA/VEGFR2 expression and suppresses tumor growth in glioblastoma xenografts. *Invest. New Drugs* 34, 24–40.
- (6) Hau, A. M., Greenwood, J. A., Löhr, C. V., Serrill, J. D., Proteau, P. J., Ganley, I. G., McPhail, K. L., and Ishmael, J. E. (2013) Coibamide A induces mTOR-independent autophagy and cell death in human glioblastoma cells. *PLoS One* 8, No. e65250.
- (7) Yao, G., Wang, W., Ao, L., Cheng, Z., Wu, C., Pan, Z., Liu, K., Li, H., Su, W., and Fang, L. (2018) Improved Total Synthesis and Biological Evaluation of Coibamide A Analogues. *J. Med. Chem.* 61, 8908–8916.
- (8) Yao, G., Pan, Z., Wu, C., Wang, W., Fang, L., and Su, W. (2015) Efficient Synthesis and Stereochemical Revision of Coibamide A. *J. Am. Chem. Soc.* 137, 13488–13491.
- (9) Nabika, R., Suyama, T. L., Hau, A. M., Misu, R., Ohno, H., Ishmael, J. E., McPhail, K. L., Oishi, S., and Fujii, N. (2015) Synthesis and biological evaluation of the [D-MeAla(11)]-epimer of coibamide A. *Bioorg. Med. Chem. Lett.* 25, 302–306.
- (10) Sable, G. A., Park, J., Kim, H., Lim, S.-J., Jang, S., and Lim, D. (2015) Solid-Phase Total Synthesis of the Proposed Structure of Coibamide A and Its Derivative: Highly Methylated Cyclic Depsipeptides. *Eur. J. Org. Chem.* 2015, 7043–7052.
- (11) Luesch, H., Chanda, S. K., Raya, R. M., DeJesus, P. D., Orth, A. P., Walker, J. R., Izpisua Belmonte, J. C., and Schultz, P. G. (2006) A functional genomics approach to the mode of action of apratoxin A. *Nat. Chem. Biol.* 2, 158–167.
- (12) Rapoport, T. A., Li, L., and Park, E. (2017) Structural and Mechanistic Insights into Protein Translocation. *Annu. Rev. Cell Dev. Biol.* 33, 369–390.
- (13) Klausner, R. D., Donaldson, J. G., and Lippincott-Schwartz, J. (1992) Brefeldin A: insights into the control of membrane traffic and organelle structure. *J. Cell Biol.* 116, 1071–1080.
- (14) Paatero, A. O., Kelloso, J., Dunyak, B. M., Almaliti, J., Gestwicki, J. E., Gerwick, W. H., Taunton, J., and Paavilainen, V. O. (2016) Apratoxin Kills Cells by Direct Blockade of the Sec61 Protein Translocation Channel. *Cell Chem. Biol.* 23, 561–566.
- (15) Baron, L., Paatero, A. O., Morel, J.-D., Impens, F., Guenin-Macé, L., Saint-Auret, S., Blanchard, N., Dillmann, R., Niang, F., Pellegrini, S., Taunton, J., Paavilainen, V. O., and Demangel, C. (2016) Mycolactone subverts immunity by selectively blocking the Sec61 translocon. *J. Exp. Med.* 213, 2885–2896.
- (16) Junne, T., Wong, J., Studer, C., Aust, T., Bauer, B. W., Beibel, M., Bhullar, B., Bruccoleri, R., Eichenberger, J., Estoppey, D., Hartmann, N., Knapp, B., Krastel, P., Melin, N., Oakeley, E. J., Oberer, L., Riedl, R., Roma, G., Schuierer, S., Petersen, F., Tallarico, J. A., Rapoport, T. A., Spiess, M., and Hoepfner, D. (2015) Decatransin, a new natural product inhibiting protein translocation at the Sec61/SecYEG translocon. *J. Cell Sci.* 128, 1217–1229.
- (17) Mackinnon, A. L., Paavilainen, V. O., Sharma, A., Hegde, R. S., and Taunton, J. (2014) An allosteric Sec61 inhibitor traps nascent transmembrane helices at the lateral gate. *eLife* 3, No. e01483.
- (18) Dejeans, N., Manié, S., Hetz, C., Bard, F., Hupp, T., Agostinis, P., Samali, A., and Chevet, E. (2014) Addicted to secrete - novel concepts and targets in cancer therapy. *Trends Mol. Med.* 20, 242–250.
- (19) Besemer, J., Harant, H., Wang, S., Oberhauser, B., Marquardt, K., Foster, C. A., Schreiner, E. P., de Vries, J. E., Dascher-Nadel, C., and Lindley, I. J. D. (2005) Selective inhibition of cotranslational translocation of vascular cell adhesion molecule 1. *Nature* 436, 290–293.
- (20) Garrison, J. L., Kunkel, E. J., Hegde, R. S., and Taunton, J. (2005) A substrate-specific inhibitor of protein translocation into the endoplasmic reticulum. *Nature* 436, 285–289.
- (21) Maifeld, S. V., MacKinnon, A. L., Garrison, J. L., Sharma, A., Kunkel, E. J., Hegde, R. S., and Taunton, J. (2011) Secretory protein profiling reveals TNF- α inactivation by selective and promiscuous Sec61 modulators. *Chem. Biol.* 18, 1082–1088.
- (22) Hall, B. S., Hill, K., McKenna, M., Ogbuchi, J., High, S., Willis, A. E., and Simmonds, R. E. (2014) The pathogenic mechanism of the *Mycobacterium ulcerans* virulence factor, mycolactone, depends on blockade of protein translocation into the ER. *PLoS Pathog.* 10, No. e1004061.
- (23) George, K. M., Chatterjee, D., Gunawardana, G., Welty, D., Hayman, J., Lee, R., and Small, P. L. (1999) Mycolactone: a polyketide toxin from *Mycobacterium ulcerans* required for virulence. *Science* 283, 854–857.
- (24) Zong, G., Hu, Z., O'Keefe, S., Tranter, D., Iannotti, M. J., Baron, L., Hall, B., Corfield, K., Paatero, A. O., Henderson, M. J., Roboti, P., Zhou, J., Sun, X., Govindarajan, M., Rohde, J. M., Blanchard, N., Simmonds, R., Inglese, J., Du, Y., Demangel, C., High, S., Paavilainen, V. O., and Shi, W. Q. (2019) Ipomoeassin F Binds Sec61 α to Inhibit Protein Translocation. *J. Am. Chem. Soc.* 141, 8450–8461.
- (25) Gamayun, I., O'Keefe, S., Pick, T., Klein, M.-C., Nguyen, D., McKibbin, C., Piacenti, M., Williams, H. M., Flitsch, S. L., Whitehead, R. C., Swanton, E., Helms, V., High, S., Zimmermann, R., and Cavalie, A. (2019) Eeyarestatin Compounds Selectively Enhance Sec61-Mediated Ca²⁺ Leakage from the Endoplasmic Reticulum. *Cell Chem. Biol.* 26, 571–583 e6.
- (26) MacKinnon, A. L., Garrison, J. L., Hegde, R. S., and Taunton, J. (2007) Photo-leucine incorporation reveals the target of a cyclopeptide inhibitor of cotranslational translocation. *J. Am. Chem. Soc.* 129, 14560–14561.
- (27) He, W., Qiu, H.-B., Chen, Y.-J., Xi, J., and Yao, Z.-J. (2014) Total synthesis of proposed structure of coibamide A, a highly N- and O-methylated cytotoxic marine cyclopeptide. *Tetrahedron Lett.* 55, 6109–6112.
- (28) Huang, K.-C., Chen, Z., Jiang, Y., Akare, S., Kolber-Simonds, D., Condon, K., Agoulnik, S., Tendyke, K., Shen, Y., Wu, K.-M., Mathieu, S., Choi, H.-W., Zhu, X., Shimizu, H., Kotake, Y., Gerwick, W. H., Uenaka, T., Woodall-Jappe, M., and Nomoto, K. (2016) Apratoxin A Shows Novel Pancreas-Targeting Activity through the Binding of Sec 61. *Mol. Cancer Ther.* 15, 1208–1216.
- (29) Van Puyenbroeck, V., and Vermeire, K. (2018) Inhibitors of protein translocation across membranes of the secretory pathway: novel antimicrobial and anticancer agents. *Cell. Mol. Life Sci.* 75, 1541–1558.
- (30) Sharma, A., Mariappan, M., Appathurai, S., and Hegde, R. S. (2010) In Vitro Dissection of Protein Translocation into the Mammalian Endoplasmic Reticulum, in *Protein Secretion: Methods and Protocols* (Economou, A., Ed.), pp 339–363, Humana Press, Totowa, NJ.
- (31) Chitwood, P. J., Juszkiwicz, S., Guna, A., Shao, S., and Hegde, R. S. (2018) EMC Is Required to Initiate Accurate Membrane Protein Topogenesis. *Cell* 175, 1507–1519 e16.
- (32) Kapoor, T. M., and Miller, R. M. (2017) Leveraging Chemotype-Specific Resistance for Drug Target Identification and Chemical Biology. *Trends Pharmacol. Sci.* 38, 1100–1109.
- (33) Chen, Q.-Y., Liu, Y., Cai, W., and Luesch, H. (2014) Improved total synthesis and biological evaluation of potent apratoxin S4 based anticancer agents with differential stability and further enhanced activity. *J. Med. Chem.* 57, 3011–3029.
- (34) Gonzalez-Teuber, V., Albert-Gasco, H., Auyeung, V. C., Papa, F. R., Mallucci, G. R., and Hetz, C. (2019) Small Molecules to Improve ER Proteostasis in Disease. *Trends Pharmacol. Sci.* 40, 684–695.
- (35) Vermeire, K., Bell, T. W., Van Puyenbroeck, V., Giraut, A., Noppen, S., Liekens, S., Schols, D., Hartmann, E., Kalies, K.-U., and Marsh, M. (2014) Signal peptide-binding drug as a selective inhibitor of co-translational protein translocation. *PLoS Biol.* 12, No. e1002011.
- (36) Ruiz-Saenz, A., Sandhu, M., Carrasco, Y., Maglathlin, R. L., Taunton, J., and Moasser, M. M. (2015) Targeting HER3 by interfering with its Sec61-mediated cotranslational insertion into the endoplasmic reticulum. *Oncogene* 34, 5288–5294.

(37) Cai, W., Ratnayake, R., Gerber, M. H., Chen, Q.-Y., Yu, Y., Derendorf, H., Trevino, J. G., and Luesch, H. (2019) Development of apratoxin S10 (Apra S10) as an anti-pancreatic cancer agent and its preliminary evaluation in an orthotopic patient-derived xenograft (PDX) model. *Invest. New Drugs* 37, 364–374.

(38) Shoemaker, R. H. (2006) The NCI60 human tumour cell line anticancer drug screen. *Nat. Rev. Cancer* 6, 813–823.

(39) Zong, G., Whisenhunt, L., Hu, Z., and Shi, W. Q. (2017) Synergistic Contribution of Tiglate and Cinnamate to Cytotoxicity of Ipomoeassin F. *J. Org. Chem.* 82, 4977–4985.

(40) Chen, Q.-Y., Liu, Y., and Luesch, H. (2011) Systematic Chemical Mutagenesis Identifies a Potent Novel Apratoxin A/E Hybrid with Improved in Vivo Antitumor Activity. *ACS Med. Chem. Lett.* 2, 861–865.

(41) Guenin-Macé, L., Baron, L., Chany, A.-C., Tresse, C., Saint-Auret, S., Jönsson, F., Le Chevalier, F., Bruhns, P., Bismuth, G., Hidalgo-Lucas, S., Bisson, J.-F., Blanchard, N., and Demangel, C. (2015) Shaping mycolactone for therapeutic use against inflammatory disorders. *Sci. Transl. Med.* 7, 289ra85.

(42) Gutiérrez, M., Suyama, T. L., Engene, N., Wingerd, J. S., Matainaho, T., and Gerwick, W. H. (2008) Apratoxin D, a potent cytotoxic cyclodepsipeptide from papua new guinea collections of the marine cyanobacteria *Lyngbya majuscula* and *Lyngbya sordida*. *J. Nat. Prod.* 71, 1099–1103.

(43) Vermeire, K., Allan, S., Provinciael, B., Hartmann, E., and Kalies, K.-U. (2015) Ribonuclease-neutralized pancreatic microsomal membranes from livestock for in vitro co-translational protein translocation. *Anal. Biochem.* 484, 102–104.

(44) Jafari, R., Almqvist, H., Axelsson, H., Ignatushchenko, M., Lundbäck, T., Nordlund, P., and Martinez Molina, D. (2014) The cellular thermal shift assay for evaluating drug target interactions in cells. *Nat. Protoc.* 9, 2100–2122.